Taylor & Francis
Taylor & Francis Group

Journal of Toxicology and Environmental Health, Part A
Current Issues

ISSN: 1528-7394 (Print) 1087-2620 (Online) Journal homepage: www.tandfonline.com/journals/uteh20

Characterization of engineered stone dust-induced reactive oxygen species generation and cytotoxicity *in vitro*

W. Kyle Mandler, Alycia K. Knepp, Stephen S. Leonard, Walter McKinney, Sarah Keeley & Yong Qian

To cite this article: W. Kyle Mandler, Alycia K. Knepp, Stephen S. Leonard, Walter McKinney, Sarah Keeley & Yong Qian (2026) Characterization of engineered stone dust-induced reactive oxygen species generation and cytotoxicity *in vitro*, Journal of Toxicology and Environmental Health, Part A, 89:7, 304-314, DOI: 10.1080/15287394.2025.2562482

To link to this article: https://doi.org/10.1080/15287394.2025.2562482

View supplementary material

Published online: 10 Oct 2025.

Submit your article to this journal

Article views: 106

View related articles

View Crossmark data

Full Terms & Conditions of access and use can be found at
https://www.tandfonline.com/action/journalInformation?journalCode=uteh20

JOURNAL OF TOXICOLOGY AND ENVIRONMENTAL HEALTH, PART A
2026, VOL. 89, NO. 7, 304–314
https://doi.org/10.1080/15287394.2025.2562482

Taylor & Francis
Taylor & Francis Group

Check for updates

Characterization of engineered stone dust-induced reactive oxygen species generation and cytotoxicity *in vitro*

W. Kyle Mandler, Alycia K. Knepp, Stephen S. Leonard, Walter McKinney, Sarah Keeley, and Yong Qian

Health Effects Laboratory Division (HELD), National Institute for Occupational Safety and Health (NIOSH), Centers for Disease Control and Prevention (CDC), Morgantown, WV, USA

ABSTRACT

Engineered stone (ES) fabrication generates respirable dust containing crystalline silica (CS), linked to accelerated silicosis outbreaks. Mechanisms underlying this toxicity, particularly the role of particle aging, remain unclear. In the occupational setting, workers are exposed to engineered stone dust (ESD) upon generation by cutting and grinding ES; however, ESD-initiated toxicity is frequently studied in labs using aged particles. This study aimed to compare radical generation and *in vitro* cytotoxicity of fresh versus aged ESD. Three different respirable ES types (ES A: 60% CS; B: 20%; C: 0%), granite (30%), and Min-u-Sil 5 (MS5, 99.5%) were generated using an automated cutting system and analyzed either freshly stored under N_2 at −80°C or after aging in air at room temperature for 2 weeks. RAW 264.7 macrophages were exposed to particles (10 µg/well, 100 µg/ml, 31.25 µg/cm^2, 24 hr), and viability, apoptosis, necrosis, and intracellular reactive oxygen species (ROS) were measured. Fresh ESD/granite exhibited significantly higher electron paramagnetic resonance (EPR) radical signals than aged counterparts and MS5. Fresh ES/granite reduced macrophage viability, while aged materials/MS5 did not. Apoptosis increased with all particles where fresh/aged difference occurred only in ES B. Necrosis rose markedly with fresh ES A. Intracellular ROS was elevated by some materials, but N-acetylcysteine (NAC) antioxidant failed to prevent cytotoxicity induced by fresh particles. In conclusion, freshly generated ESD displayed greater radical-generating capacity and distinct cytotoxic effects compared to aged ESD, influenced by factors beyond CS content. ROS-independent mechanisms appear crucial for acute cytotoxicity. These findings indicate particle aging as a critical factor in ESD toxicological assessment.

Introduction

Engineered stone (ES), also known by various names such as artificial stone, composite stone, or quartz surfacing, has become a widely favored material in the construction and design industries (Mandler, Qi, and Qian 2023; Ramkissoon et al. 2024). Engineered stone popularity stems from its architectural versatility, esthetic appeal, and often a more competitive price point compared to natural stone options (Ramkissoon et al. 2024). Primarily utilized for kitchen and bathroom countertops, ES offers a consistent appearance and enhanced durability; however, it is distinguishable from natural stone by its composition. Unlike natural stones such as granite, which typically contains 30–50% silica, or marble, with a silica content of less than 10%, ES is characterized by an exceptionally high concentration of crystalline silica, with concentrations sometimes exceeding 90% by weight (Ramkissoon et al. 2024). This silica is bound together using organic resin binders, with the overall silica content reported to range from 56% to as high as 95% in some analyses (DeVaughn et al. 2025). The disparity in silica content compared to natural alternatives suggests a potential for increased adverse health risks associated with ES, particularly concerning the generation of respirable dust during the fabrication processes such as grinding, cutting, and sanding (DeVaughn et al. 2025). The marked differences in silica content between ES and natural stone (90% vs. <50%) suggest a potentially disproportionate adverse health risk associated with exposure to ESD (OSHA 2015). A material with significantly higher silica content might conceivably generate dust with a higher concentration of the harmful agent, crystalline silica,

CONTACT W. Kyle Mandler wmandler@cdc.gov Pathology and Physiology Branch, Health Effects Laboratory Division, National Institute for Occupational Safety and Health, 1095 Willowdale Road, Morgantown, WV, 26505, USA
Supplemental data for this article can be accessed online at https://doi.org/10.1080/15287394.2025.2562482
© 2025 Taylor & Francis Group, LLC

which is the known cause of silicosis (Castranova and Vallyathan 2000).

The fabrication of ES products, which includes customization of slabs for countertops and other applications, involves processes such as cutting, grinding, drilling, and polishing (Mandler, Qi, and Qian 2023). These processes inevitably generate fine dust particles, a significant portion of which falls within the respirable size range, indicating that these particles might become airborne and readily inhaled by workers in the vicinity (Thompson and Qi 2022). This generated dust contains a high (as much as 90% by mass) respirable crystalline silica (RCS) (Ramkissoon et al. 2024). Alarmingly, a growing number of ES countertop workers have been diagnosed with silicosis across the globe (Rose et al. 2019), signaling a concerning reemergence of this historically known but preventable lung disease. The widespread reporting of silicosis in ES workers across multiple countries (Fazio et al. 2023; Kramer et al. 2012; Ronsmans et al. 2018) indicates a significant and systemic occupational health problem, rather than isolated incidents.

Silica, a naturally occurring mineral, exists in various crystalline and amorphous forms and is widely utilized in industry, leading to occupational and environmental exposure (Liu and Sayes 2022). The diverse applications of silica, ranging from construction and mining to the manufacturing of ceramics and abrasives, increase the likelihood of inhalation of silica particles and subsequent risk to respiratory health (Arnoldussen et al. 2019). The adverse health hazards associated with silica exposure are influenced by the physicochemical properties of the particles, including their diameter, shape, surface area, and surface reactivity (Liu and Sayes 2022). Inhalation of fine silica particles may lead to severe and irreversible lung diseases such as silicosis and pulmonary fibrosis, characterized by inflammation and scarring of the lung tissue, ultimately impairing respiratory function (B. Yang et al. 2025).

The principal risk associated with ES comes from inhaling freshly generated RCS particles during fabrication, as their newly fractured surfaces are highly reactive (Castranova et al. 2002). Over time, these particles undergo surface modifications through processes including hydration, adsorption, and reduction, which markedly decrease their chemical reactivity and, therefore, their toxicity compared to fresh-samples (Vallyathan et al. 1988; J. Yang and Wang 2006). The crucial initial biological events that drive silicosis development, including the rapid formation of reactive oxygen species (ROS), lipid membrane damage (peroxidation) (Vallyathan et al. 1988), DNA fragmentation (Thibodeau et al. 2004), and triggering of various inflammatory responses (Fubini and Hubbard 2003; Hornung et al. 2008) occur immediately following exposure to these potent, freshly fractured RCS particles. Castranova (1994) provided direct evidence that freshly ground crystalline silica is a more potent stimulant of alveolar macrophages than aged silica *in vivo*. Data suggest that the initial state of the particle may be attributed to surface radicals, which produce a more potent inflammatory response.

The aim of the present study was to examine the effects of particle aging on several biomarkers indicative of *in vitro* toxicity. It was postulated that fresh ESD, similar to that which workers may be exposed, might demonstrate significantly higher ROS generation capacity than aged controls, resulting in enhanced cytotoxicity of fresh particles compared to particles that were allowed to age prior to exposure. To investigate the cytotoxic and oxidative effects of ESD, the RAW 264.7 murine macrophage cell line was selected. This selection is justified based upon the key role of alveolar macrophages as the first line of cellular defense against inhaled particulates in the lung. These RAW 264.7 cells are responsible for phagocytosing foreign materials and initiating the inflammatory and fibrotic responses characteristic of diseases like silicosis (Hamilton, Thakur, and Holian 2008). The RAW 264.7 cell line is a well-established and widely accepted *in vitro* model for inhalation toxicology testing because these cells retain critical macrophage functions, including phagocytosis, respiratory burst activity, and production of inflammatory mediators (Claudio et al. 1995; Mischler et al. 2016, Leonard et al. 2000).

Methods

Particle generation, collection, and aging

Particles were generated in real-time using a custom-built automated countertop particle generation system. Briefly, the system operates by advancing a circular saw with a stone cutting disc that cuts off the end of the countertop slab, generating an aerosol. The saw is retracted and the ES slab advanced by one disc width before the start of the next cut. This cutting assembly was placed inside an air-tight stainless-steel chamber with a HEPA filter inlet port, and aerosols exited the chamber at a flow rate of 30 L/min. This exit port was positioned approximately 30 cm from the saw. After leaving the cutting assembly chamber, the aerosol passed through a cyclone with a cut size of 5 μm aerodynamic diameter to ensure collection of respirable dust. After the cyclone, the aerosol was collected on a Teflon filter. The air flow was controlled by a mass flow controller connected to house vacuum. The cutting process was repeated for 3 hr then the material was collected from the filter by scraping using a sterile cell scraper. The filters were replaced between each collection period. Following collection, the particles were stored under 99% nitrogen gas and at −80°C in a 3 ml glass vial. The 3-hr collection runs were repeated until a sufficient (more than 1 g) amount of dust was collected. Following isolation, a subset of each respirable dust was then stored under normal atmosphere in an identical sealed glass container at room temperature, while the rest remained stored under 99% N_2 at −80°C for 2 weeks. Three types of ES materials (ES A, B, and C) were employed in this study, as well as natural granite rock and Min-u-sil-5 (MS5), as a CS positive control. The CS content was previously determined utilizing X-ray diffraction analysis according to NIOSH Method 7500 as described in Thompson and Qi (2022). The CS content for each material was as follows: 60% (ES A), 20% (ES B), 0% (ES C), 30% (granite), or 99.5% (MS5).

Electron paramagnetic resonance

To assess free radical generation in an acellular environment, electron paramagnetic resonance (EPR) spin-trapping was employed. Engineered stone samples were exposed to hydrogen peroxide (H_2O_2) to induce a Fenton-like reaction and generate hydroxyl radicals (•OH). 5,5-Dimethyl-1-pyrroline N-oxide (DMPO) (100 mM) was used as a spin trap. Samples were mixed in phosphate buffered saline (PBS), filtered to halt the reaction, and analyzed using an EPR spectrometer. Signal intensity from the characteristic 1:2:2:1 DMPO-OH• adduct spectrum was utilized to quantify relative radical production. To assess free radical generation in the presence of cells, the experiment was repeated with RAW 264.7 (American Type Culture Collection, Manassas, Virginia) cells added to the PBS.

Cytotoxicity assessment via high content imaging

The murine macrophage cell line RAW 264.7 was maintained in Dulbecco's Modified Eagle Medium (DMEM) supplemented with 10% fetal bovine serum (FBS), 2 mM L-glutamine, and antibiotics (100 U/ml penicillin and 100 μg/ml streptomycin). Cultures were kept in a humidified incubator at 37°C with 5% CO_2 and were subcultured every 3 days upon reaching confluence. Cells were seeded on 96-well plates at 40,000 cells/well in clear DMEM. Twenty-four hr after seeding, 10 μg fresh or aged ESD, or Min-u-Sil 5 (positive control) added to each well and incubated for 24 hr. A single, sub-lethal dose was selected based upon preliminary range-finding experiments, as this enabled detection of differences in cytotoxic mechanisms such as apoptosis vs. necrosis that may be masked by overwhelming cell death at higher doses. Two technical replicates were used per experiment, and the experiments were repeated for a total of $n = 4–9$. Twenty-four hr following exposure, each well was incubated with a cocktail containing CellEvent™ Caspase-3/7 Green Detection Reagent and Propidium Iodide (PI). In all cases, Hoechst 33,342 was used as a nuclear stain. After a 30-min incubation period, plates were imaged using a ImageXpress Micro XLS high content imaging platform. Representative images from the high-content imaging process can be seen in Figure 1.

To determine the contribution of ROS to toxicity, an additional experiment was conducted wherein cells were incubated with 10 μg fresh

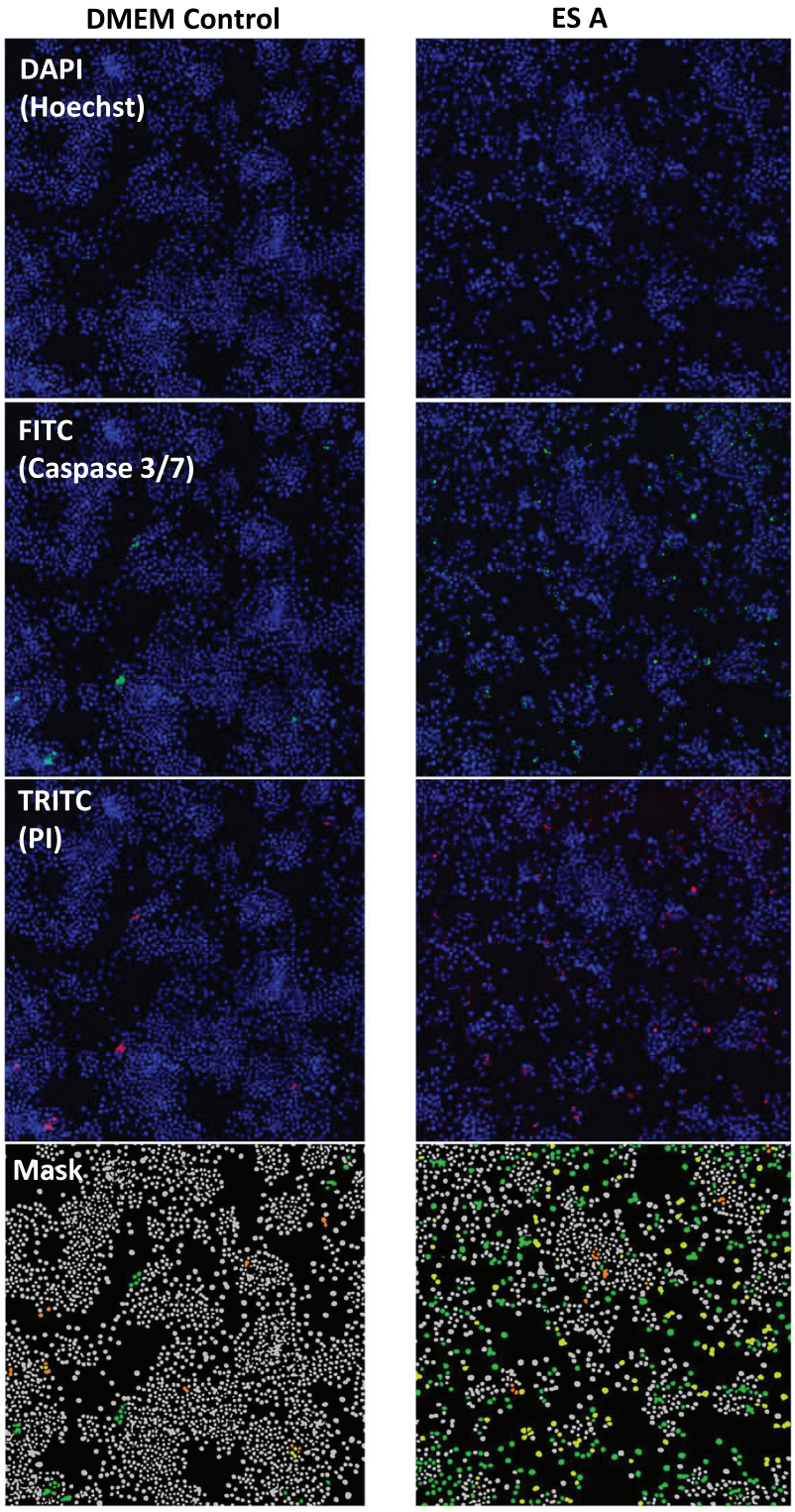

FIGURE 1. Representative high-content microscopy images of RAW 264.7 cells after 24-h exposure to either a negative DMEM control (left) or ES a (right). Cells were stained with Hoechst (blue, nuclei), Caspase 3/7 (green, apoptosis marker), and propidium iodide (red, necrosis/late apoptosis marker). "Mask" images show cells positive for one or both dyes: green (Caspase 3/7), orange (propidium iodide), and yellow (both Caspase 3/7 and propidium iodide).

ESD alone or in the presence of 100 μM of N-acetyl cysteine (NAC) for 24 hr. Following the 24 hr incubation period, the ROS-sensitive dye CellRox Deep Red was added to each well and plates imaged after 30 min. For all wells, nine images were taken, and the average number of living cells, cells positive for each stain, and total cell area were measured.

Statistics

All data are presented as mean ± standard deviation (SD). Statistical analyses were conducted using GraphPad Prism software (Version 9.0, La Jolla, CA). Data were first tested for normal distribution using the D'Agostino-Pearson normality test. Subsequently, an ordinary one-way analysis of variance (ANOVA) was performed to determine overall statistical significance among the groups. To specifically compare each treatment group against the vehicle (DMEM) control group, Dunnett's multiple comparisons test was used. A p-value <0.05 was considered statistically significant for all tests.

Results

After 24 hr incubation, the number of living cells was significantly reduced in wells treated with fresh dust from all ES materials and granite compared to DMEM control. In contrast, treatment with any of the aged materials or with MS5 did not result in a significant change in cell viability. Despite the overall decrease in cell number per well, total cell area was elevated in wells containing fresh granite only (Figures 2(A-B)). The % counted cells positive for Caspase 3/7 dye, an indicator of apoptosis, was enhanced significantly for all materials compared to control and only ES B exhibited a difference between fresh and aged (Figure 2(C)). Cells positive for PI, an indicator of necrosis, were increased only in fresh ES A (Figure 2(D)). The % cells positive for CellRox Red, an indicator of oxidative stress, were markedly greater in both fresh and aged ES A and aged ES B (Figure 3). The addition of 100 μM NAC to wells containing cells incubated with fresh particles was tested to determine the contribution of ROS to previously observed cytotoxicity. Despite similar patterns of changes in cell

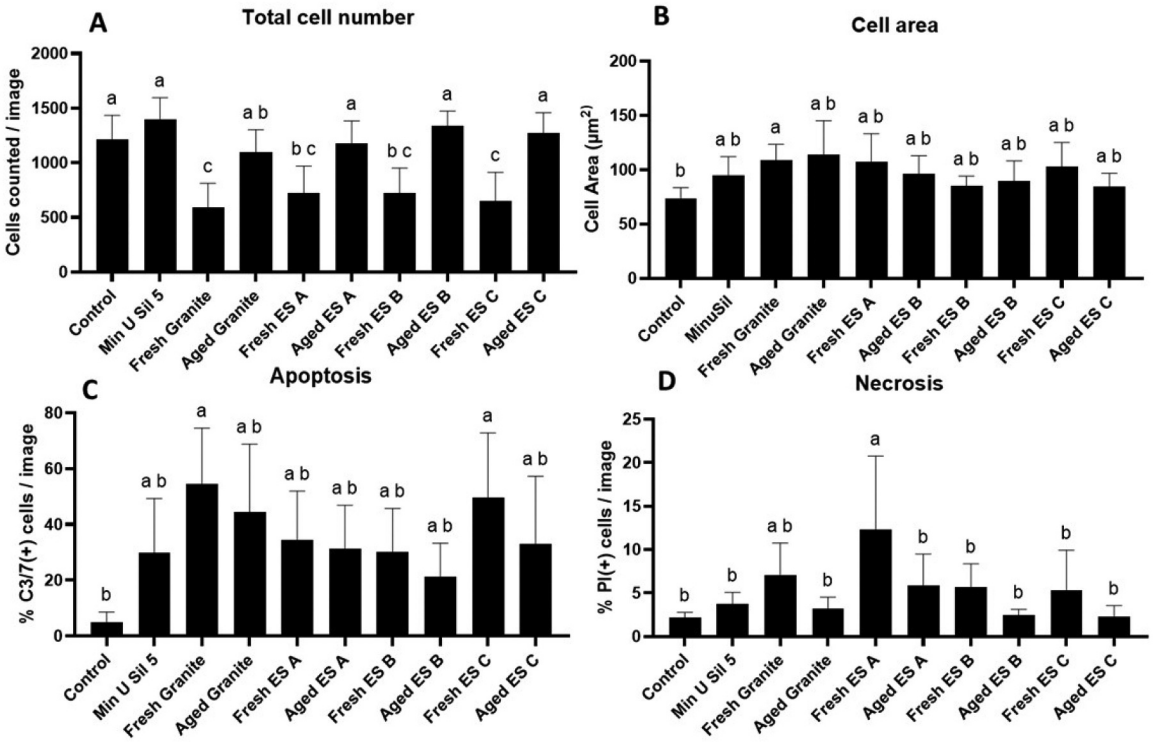

FIGURE 2. Measurements of cell number, area, apoptosis, and necrosis. (A) Total cell number per image. (B) Total cell area per image. (C) Apoptosis, assessed by the percentage of Caspase 3/7(+) cells per image. (D) Necrosis, assessed by the percentage of propidium iodide (+) cells per image. Bars represent means ± SD ($N = 5–7$). Different letters above bars indicate significant differences between groups ($p < 0.05$). Letters a, b, and c each represent a group of means that are not significantly different from each other.

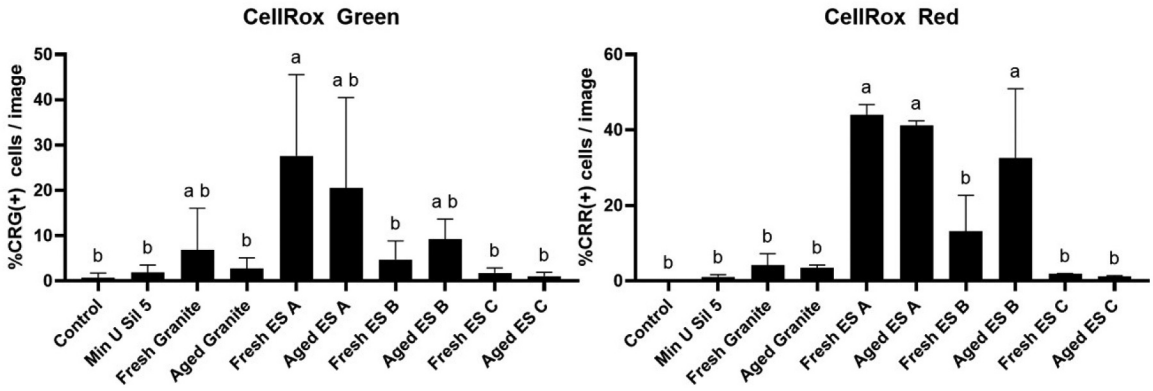

FIGURE 3. (Left) percentage of CelRox Green (CRG) positive cells per image. This indicates general oxidative stress. (Right) Percentage of CellRox red (CRR) positive cells per image. This indicates specifically mitochondrial oxidative stress. Data are presented as mean ± standard deviation. Bar heights represent mean values ± SD. Letters a, b, and c each represent a group of means that are not significantly different from each other ($p < 0.05$). $N = 4$.

viability, apoptosis, and necrosis, the presence of NAC exerted no significant effect (Figure 5).

The average EPR spectra peak intensity for each fresh material are as follows (units are EPR peak height in mm ± SD): Background: 23 ± 2., MS5: 33 ± 4., Granite 71 ± 3.5, ES A 89 ± 3.1, ES B 61 ± 2.5, and ES C: 44 ± 4.2 (Figure 4). The spectra peak intensity for all materials was significantly greater than background, and each fresh countertop material was greater than MS5. Following aging, the peak intensities were granite: 59 ± 4.7, ES A: 61 ± 4.7, ES B 33 ± 3.1, ES C 30 ± 4.2. All aged materials demonstrated less intense peaks compared to their fresh counterparts, and all were above background. Aged granite and ES A peaks were still significantly larger than MS5. In the presence of RAW 264.7 cells, the spectra peak intensity for each fresh material is as follows: background: 8.6 ± 1.5, MS5: 10 ± 1, granite 30 ± 3.7, ES A 32 ± 2.1, ES B 15 ± 1, and ES C: 16 ± 1.4. Granite, ES A, and ES C were significantly greater than background. Following aging, the peak intensities were granite: 17 ± 1, ES A: 18.3 ± 2.1, ES B 10 ± 1.0, ES C 9.7 ± 1.5. EPR spectra from granite and ES A were significantly greater than background and significantly reduced compared to fresh.

Discussion

Our previous *in vivo* study investigated the pulmonary toxicity of ES dusts with CS content in rats following intratracheal instillation {Mandler, pers. comm.}. Findings demonstrated pulmonary inflammation, persistent cellular injury as indicated by elevated BALF LDH activity and inflammatory cell counts, and progressive fibrosis, with effects most pronounced following exposure to high-CS ES (ES A, 60%) and pure silica (MS5), and least severe with CS-free ES (ES C). Histopathological analysis confirmed these observations, demonstrating severe alveolitis, granulomatous inflammation, and marked fibrosis primarily in the MS5 and ES A groups by 84 d post-exposure, in conjunction with associated systemic effects observed via hematological analysis. Crucially, linear regression indicated that while CS content was a major driver of toxicity, various trace metals present in the ES dusts also significantly contributed to the observed adverse outcomes, suggesting a complex toxicological profile beyond silica alone. However, a significant limitation was the use of aged, bulk particle samples, which may possess altered physicochemical properties and reduced reactivity compared to freshly generated particles that workers inhale, potentially underestimating the true toxicity. Despite this constraint, the study clearly demonstrates the potent inflammatory and fibrogenic potential following ESD exposure, emphasizing significant potential occupational health risks and indicating the contributing role of both silica and trace metals.

Building upon previous *in vivo* investigations, the current research addressed a key limitation: the potentially heightened toxicity of freshly generated particles encountered by workers in the

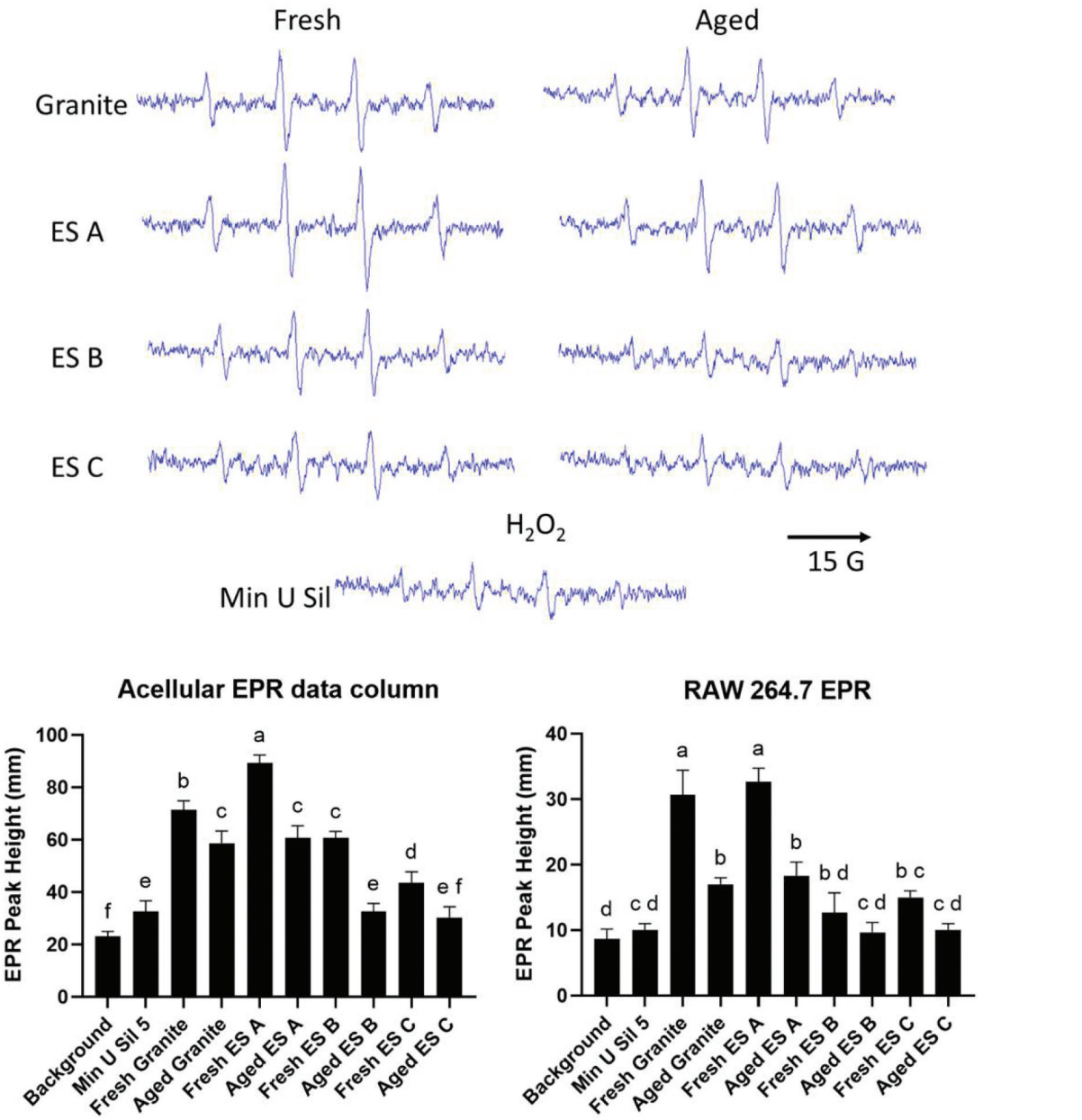

FIGURE 4. (Top) Representative EPR spectra comparing fresh (left panels) and aged (right panels) samples of granite, ES A, ES B, ES C, and Min-U-Sil 5. (Bottom) Peak magnitude for each material in an acellular environment (left) and in the presence of RAW 264.7 cells (right). Bar heights represent mean values ± SD, $N = 3$. ($p < 0.05$). Letters a, b, and c each represent a group of means that are not significantly different from each other.

course of production activities like cutting and grinding {Mandler, pers. comm.}. It was postulated that freshly generated ESD might initiate greater ROS generation capacity and induce more pronounced cytotoxicity compared to aged equivalents, mirroring the known higher reactivity of freshly fractured silica.

The electron paramagnetic resonance (EPR) analysis clearly demonstrated that freshly generated dusts from all ES types (ES A, B, C) and natural granite produced significantly higher levels of hydroxyl radicals (•OH) in an acellular Fenton-like reaction system compared to their aged counterparts (Figure 4). This is in agreement with the established understanding that freshly fractured silica surfaces possess unstable bonds and surface radicals (silanols, silyl radicals) that readily engage in oxidation-reduction processes, generating ROS (Vallyathan et al. 1988). Notably, fresh ES A (60% CS) and fresh granite (30% CS) exhibited the

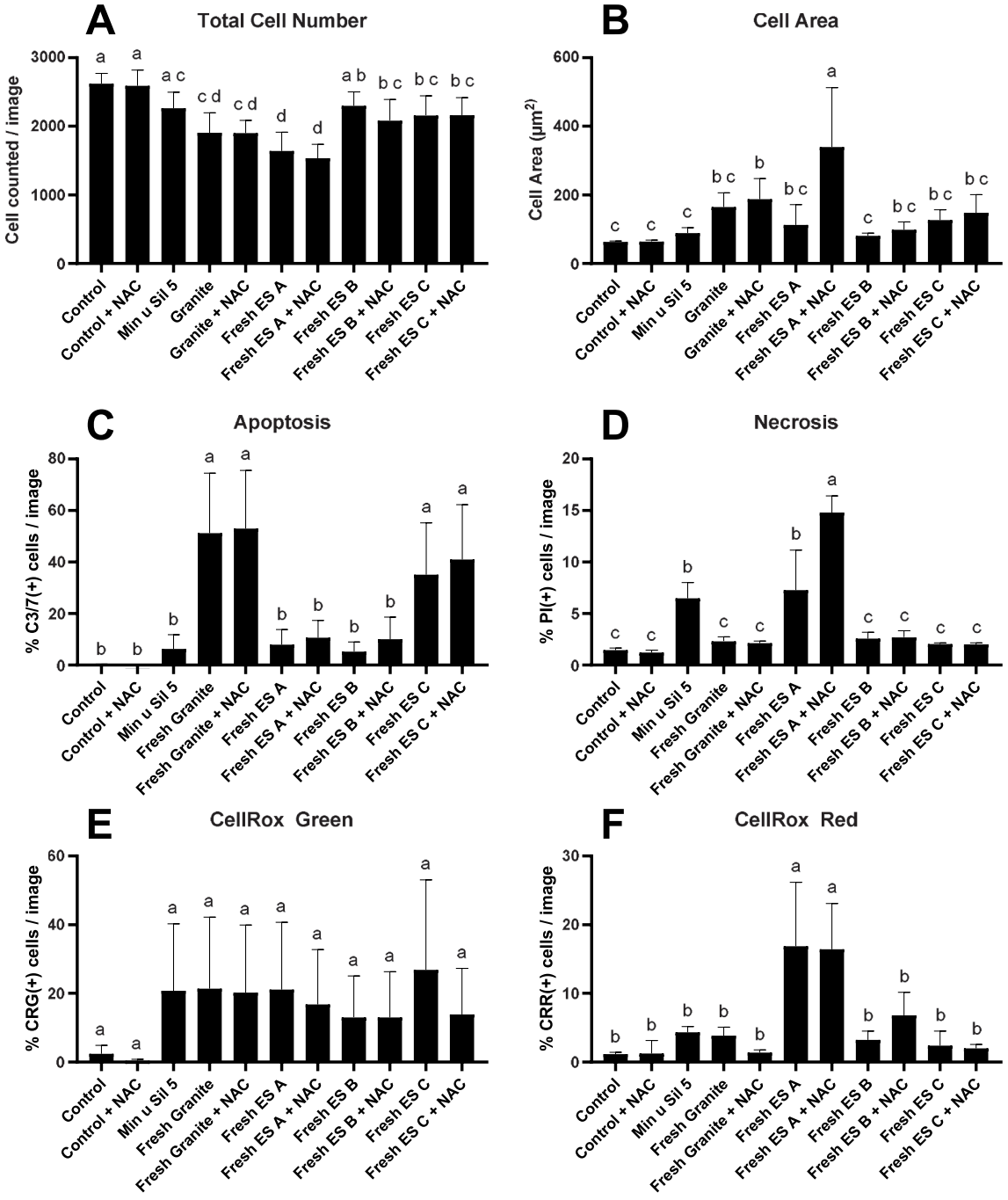

FIGURE 5. (A) Total cell number and (B), cell area per image following exposure to fresh ESD or fresh ESD with the antioxidant N-acetyl cysteine. (C) Apoptosis, assessed by % Caspase 3/7(+) cells per image. (D) Necrosis, assessed by % propidium iodide (+) cells per image (E) % CellRox green (CRG) positive cells per image. This indicates general oxidative stress. (F) Percentage of CellRox red (CRR) positive cells per image. Bar heights represent mean values ± SD. Letters a, b, and c each represent a group of means that are not significantly different from each other ($p < 0.05$). $N = 5–9$.

highest acellular radical generation, surpassing even MS5, suggesting that elements other than simply CS content, potentially including surface characteristics affected by the resin binder or the existence of particular transition metals within the ES matrix, play a major role in this initial reactivity. The significant reduction in EPR signal intensity after 2 weeks of aging under ambient conditions confirms the transient nature of this hyper-reactivity, as surface sites likely undergo hydration, reduction, or other modifications (Albrecht et al. 2005; Fubini et al. 1990). A similar pattern of

enhanced radical generation by fresh particles, particularly ES A and granite, was noted in the presence of RAW 264.7 cells, indicating that this inherent reactivity translates to a biological context.

This heightened reactivity of fresh particles correlated directly with acute cytotoxicity. Exposure to fresh ES A, ES B, ES C, and granite dusts significantly reduced viable cell numbers compared to control after 24 hr (Figure 2(A)). In contrast, aged versions of these materials, as well as MS5, did not markedly affect cell counts under these conditions. This finding has important implications, providing *in vitro* evidence that the initial interaction with freshly generated ESD poses a greater cytotoxic threat than exposure to aged dust. This observation suggests that previous toxicological assessments using aged dust, including our own *in vivo* study, may have underestimated the acute hazard potential present in occupational settings during active manufacturing steps.

However, the examination of cell death pathways revealed a nuanced situation. Although fresh ES A uniquely induced significant necrosis (PI positivity, Figure 2(D)), indicative of severe, rapid cell damage, while apoptosis (Caspase 3/7 positivity, Figure 2(C)) was elevated by all tested materials, both fresh and aged (with the minor exception of ES B showing a non-significant change). These findings suggest that while the acute cell toxicity is linked to freshness of the particles, particularly high-CS ES A, the capacity to initiate apoptosis persists even after aging. The CS-free ES C also induced apoptosis, indicating that the non-silica components are not inert and contribute to the overall biological effect. Further, the observed rise in total cell area in the fresh granite group (Figure 2(B)) might reflect macrophage activation and morphological changes in response to particle phagocytosis and stress.

Given the evidence for ROS generation and the known role of oxidative stress detected in silica toxicity (Albrecht et al. 2005; Vallyathan et al. 1988), contribution of oxidant radicals to the observed cytotoxicity was investigated using the antioxidant NAC. CellRox assays confirmed enhanced oxidative stress (CRR) in cells exposed to both fresh and aged ES A and ES B, partially in agreement with EPR results but also showing persistent effects in aged samples. However, co-incubation with NAC failed to mitigate the cytotoxicity or prevent the induction of apoptosis or necrosis initiated by fresh ESD (Figure 5). This implies that even though fresh particles generate more ROS, the overt cytotoxicity and cell death pathways measured at 24 hr may not be solely or directly dependent upon overwhelming oxidative stress, or that the damage cascade initiated by the highly reactive fresh particles is too rapid or severe to be fully prevented by NAC intervention under these experimental conditions. The failure of NAC to prevent cytotoxicity suggests that mechanisms beyond oxidative stress may be primarily responsible for the observed cell death. A key ROS-independent pathway begins after macrophage phagocytosis, where ingested silica particles physically disrupt the lysosomal membrane, leading to release of proteases such as cathepsins into the cytosol. This lysosomal rupture triggers the assembly and activation of the NLRP3 inflammasome. The inflammasome then activates caspase-1 (Hornung et al. 2008), which initiates pyroptosis by cleaving gasdermin D to form pores in the cell's plasma membrane (Kovacs and Miao 2017). This entire cascade, from physical membrane damage to inflammasome-mediated pyroptosis, might not necessarily be inhibited by an antioxidant like NAC (Cassel et al. 2008; Hamilton, Thakur, and Holian 2008).

This study has limitations inherent to *in vitro* models. RAW 264.7 cells represent a macrophage line and might not completely represent the responses of primary alveolar macrophages or the complex cellular interactions within the lung microenvironment. The single 24-hr time point and single dose might not encompass the complete dynamics of cellular response. Aging conditions were standardized but represent only one possible environmental scenario. Nevertheless, the use of a realistic particle generation system producing respirable dust and direct comparison of fresh versus aged particles provide meaningful perspective.

Conclusions

This study demonstrated that freshly generated ES dust exhibits significantly enhanced *in vitro* oxidative potential and acute cytotoxicity compared to aged dust, supporting the hypothesis that the

reactivity of particles generated during manufacturing steps poses a distinct and potentially underestimated hazard. While oxidative stress is clearly induced, its direct role in mediating the observed cell death requires further clarification, as NAC intervention was ineffective. These findings stress the importance of controlling dust exposure at the source during ES processing to minimize worker exposure to these highly reactive fresh particles and emphasize the need for risk assessments to consider the enhanced toxicity associated with particle freshness. This study warrants a future whole-body inhalation exposure to real-time ES dusts to further explore *in vivo* toxicity. Future studies need to explore earlier time points, investigate alternative cell death pathways, and further probe the interplay between silica content, metal co-contaminants, and particle aging in driving ES toxicity.

Disclaimer

The findings and conclusions in this report are those of the author(s) and do not necessarily represent the official position of the National Institute for Occupational Safety and Health (NIOSH), Centers for Disease Control and Prevention (CDC). Mention of any company or product does not constitute endorsement by NIOSH/CDC.

Disclosure statement

No potential conflict of interest was reported by the author(s).

Funding

The author(s) reported that there is no funding associated with the work featured in this article.

Data availability statement

The data that support the findings of this study are available from the corresponding author, WKM, upon reasonable request.

References

Albrecht, C., A. M. Knaapen, A. Becker, D. Höhr, P. Haberzettl, and F. J. van Schooten. 2005. "The Crucial Role of Particle Surface Reactivity in Respirable Quartz-Induced Reactive Oxygen/Nitrogen Species Formation and APE/Ref-1 Induction in Rat Lung." *Respiratory Research* 6 (1): 129. https://doi.org/10.1186/1465-9921-6-129.

Arnoldussen, Y. J., T. Kringlen Ervik, M. Baarnes Eriksen, I. Kero, V. Skaug, and S. Zienolddiny. 2019. "Cellular Responses of Industrially Relevant Silica Dust on Human Glial Cells *in Vitro*." *International Journal of Molecular Sciences* 20 (2): 358. https://doi.org/10.3390/ijms20020358.

Cassel, S. L., S. C. Eisenbarth, S. S. Iyer, J. J. Sadler, O. R. Colegio, and L. A. Tephly. 2008. "The NALP3 Inflammasome Is Essential for the Development of Silicosis." In Proceedings of the National Academy of Sciences, Vol. 105 USA: 9035–9040.

Castranova, V. 1994. "Generation of Oxygen Radicals and Mechanisms of Injury Prevention." *Environmental Health Perspectives* 102 (suppl 10): 65–68. https://doi.org/10.1289/ehp.94102s1065.

Castranova, V., D. Porter, L. Millecchia, J. Y. C. Ma, A. F. Hubbs, and A. Teass. 2002. "Effect of Inhaled Crystalline Silica in a Rat Model: Time Course of Pulmonary Reactions." *Molecular and Cellular Biochemistry* 234–235 (1): 177–184. https://doi.org/10.1023/A:1015967017103.

Castranova, V., and V. Vallyathan. 2000. "Silicosis and Coal Workers' Pneumoconiosis." *Environ. Health. Perspect* 108 (suppl 4): 675–684. DOI: 10.1289/ehp.00108s4675

Claudio, E., F. Segade, K. Wróbel, S. Ramos, and P. S. Lazo. 1995. "Activation of Murine Macrophages by Silica Particles in Vitro is a Process Independent of Silica-Induced Cell Death." *American Journal of Respiratory Cell and Molecular Biology* 13 (5): 547–554. https://doi.org/10.1165/ajrcmb.13.5.7576690.

DeVaughn, A., L. H. T. Go, R. A. Cohen, and Y. Shao. 2025. "Investigation of Occupational Exposure to Respirable Crystalline Silica (RCS) Among Engineered Stone Fabricators in Chicago—A Pilot Study." *Journal of Occupational and Environmental Hygiene* 22 (2): 101–109. https://doi.org/10.1080/15459624.2024.2421488.

Fazio, J. C., S. A. Gandhi, J. Flattery, A. Heinzerling, N. Kamangar, N. Afif. 2023. "Silicosis Among Immigrant Engineered Stone (Quartz) Countertop Fabrication Workers in California." *JAMA Internal Medicine* 183 (9): 991–998. https://doi.org/10.1001/jamainternmed.2023.3295.

Fubini, B., E. Giamello, M. Volante, and V. Bolis. 1990. "Chemical Functionalities at the Silica Surface Determining Its Reactivity When Inhaled. Formation and Reactivity of Surface Radicals." *Toxicology and Industrial Health* 6 (6): 571–598.

Fubini, B., and A. Hubbard. 2003. "Reactive Oxygen Species (ROS) and Reactive Nitrogen Species (RNS) Generation by Silica in Inflammation and Fibrosis." *Free Radical Biology and Medicine* 34 (12): 1507–1516. https://doi.org/10.1016/S0891-5849(03)00149-7.

Hamilton, R. F., S. A. Thakur, and A. Holian. 2008. "Silica Binding and Toxicity in Alveolar Macrophages." *Free*

Radical Biology and Medicine 44 (7): 1246–1258. https://doi.org/10.1016/j.freeradbiomed.2007.12.027.

Hornung, V., F. Bauernfeind, A. Halle, E. O. Samstad, H. Kono, and K. L. Rock. 2008. "Silica Crystals and Aluminum Salts Activate the NALP3 Inflammasome Through Phagosomal Destabilization." *Nature Immunology* 9 (8): 847–856. https://doi.org/10.1038/ni.1631.

Kovacs, S. B., and E. A. Miao. 2017. "Gasdermins: Effectors of Pyroptosis." *Trends Cell Biology* 27 (9): 673–684. https://doi.org/10.1016/j.tcb.2017.05.005.

Kramer, M. R., P. D. Blanc, E. Fireman, A. Amital, A. Guber, N. A. Rhahman. 2012. "Artificial Stone Silicosis: Disease Resurgence Among Artificial Stone Workers." *Chest* 142 (2): 419–424. https://doi.org/10.1378/chest.11-1321.

Leonard, S. S., S. Wang, X. Shi, B. S. Jordan, V. Castranova, and M. A. Dubick. 2000. "Wood Smoke Particles Generate Free Radicals and Cause Lipid Peroxidation, DNA Damage, Nfκb Activation and TNF-α Release in Macrophages." *Toxicology* 150 (1–3): 147–157. DOI: 10.1016/S0300-483X(00)00256-0

Liu, J. Y., and C. M. Sayes. 2022. "A Toxicological Profile of Silica Nanoparticles." *Toxicology Research* 11 (4): 565–582. https://doi.org/10.1093/toxres/tfac038.

Mandler, W. K., C. Qi, and Y. Qian. 2023. "Hazardous Dusts from the Fabrication of Countertop: A Review." *Archives of Environmental Occupational Health* 78 (2): 118–126. https://doi.org/10.1080/19338244.2022.2105287.

Mandler, W. K., C. Qi, D. Thompson, T. Crabbs, A. F. Hubbs, A. K. Knepp, S. Keeley, L. Battelli, S. A. Friend, et al. "In Review. Pulmonary Inflammatory and Fibrogenic Responses in Rats Following Intratracheal Instillation of Dusts from Natural and Engineered Stones." *Journal of Toxicology and Environmental Health*, Part A.

Mischler, S. E., E. G. Cauda, M. Di Giuseppe, L. J. McWilliams, C. S. Croix, M. Sun. 2016. "Differential Activation of RAW 264.7 Macrophages by Size-Segregated Crystalline Silica." *Journal of Occupational Medicine and Toxicology* 11 (1): 57. https://doi.org/10.1186/s12995-016-0145-2.

OSHA (Occupational Safety and Health Administration). 2015. *Worker Exposure to Silica During Countertop Manufacturing, Finishing and Installation*. Washington, DC: U.S. Department of Labor.

Ramkissoon, C., S. Gaskin, Y. Song, D. Pisaniello, and G. R. Zosky. 2024. "From Engineered Stone Slab to Silicosis: A Synthesis of Exposure Science and Medical Evidence." *International Journal of Environmental Research and Public Health* 21 (6): 683. https://doi.org/10.3390/ijerph21060683.

Ronsmans, S., L. Decoster, S. Keirsbilck, E. Verbeken, and B. Nemery. 2018. "Artificial Stone-Associated Silicosis in Belgium." *Occupational and Environmental Medicine* 76 (2): 2018. https://doi.org/10.1136/oemed-2018-105436.

Rose, C., A. Heinzerling, K. Patel, C. Sack, J. Wolff, L. Zell-Baran. 2019. "Severe Silicosis in Engineered Stone Fabrication Workers—California, Colorado, Texas, and Washington, 2017–2019." *MMWR Morbidity and Mortality Weekly Report* 68 (38): 813–818. https://doi.org/10.15585/mmwr.mm6838a1.

Thibodeau, M. S., C. Giardina, D. A. Knecht, J. Helble, and A. K. Hubbard. 2004. "Silica-Induced Apoptosis in Mouse Alveolar Macrophages is Initiated by Lysosomal Enzyme Activity." *Toxicological Sciences* 80 (1): 34–48. https://doi.org/10.1093/toxsci/kfh121.

Thompson, D., and C. Qi. 2022. "Characterization of the Emissions and Crystalline Silica Content of Airborne Dust Generated from Grinding Natural and Engineered Stones." *Annals of Work Exposures and Health* 67 (2): 266–280. https://doi.org/10.1093/annweh/wxac070.

Vallyathan, V., X. L. Shi, N. S. Dalal, W. Irr, and V. Castranova. 1988. "Generation of Free Radicals from Freshly Fractured Silica Dust. Potential Role in Acute Silica-Induced Lung Injury." *The American Review of Respiratory Disease* 138 (5): 1213–1219. https://doi.org/10.1164/ajrccm/138.5.1213.

Yang, B., X. Liu, C. Peng, X. Meng, and Q. Jia. 2025. "Silicosis: From Pathogenesis to Therapeutics." *Frontiers in Pharmacology* 16:1516200. https://doi.org/10.3389/fphar.2025.1516200.

Yang, J., and E. G. Wang. 2006. "Reaction of Water on Silica Surfaces." *Current Opinion in Solid State & Materials Science* 10 (1): 33–39. https://doi.org/10.1016/j.cossms.2006.02.001.